Phase transitions in a nonequilibrium percolation model

Siegfried Clar,[1] Barbara Drossel,[2] Klaus Schenk,[1] and Franz Schwabl[1]
[1]*Institut für Theoretische Physik, Physik-Department der Technischen Universität München, James-Franck-Straße, D-85747 Garching, Germany*
[2]*Department of Theoretical Physics, University of Manchester, Manchester M13 9PL, England*
(Received 14 February 1997)

We investigate the percolation properties of a two-state (occupied-empty) cellular automaton, where at each time step a cluster of occupied sites is removed and the same number of randomly chosen empty sites is occupied again. We find a finite region of critical behavior, formation of synchronized stripes, additional phase transitions, as well as violation of the usual finite-size scaling and hyperscaling relations, phenomena that are very different from conventional percolation systems. We explain the mechanisms behind all these phenomena using computer simulations and analytic arguments. [S1063-651X(97)07708-8]

PACS number(s): 05.70.Jk, 05.70.Ln

I. INTRODUCTION

During the past years, systems that exhibit self-organized criticality (SOC) have attracted much attention since they might explain part of the abundance of fractal structures in nature [1]. Their common features are slow driving or energy input (e.g., dropping of sand grains [1], increase of strain [2], tree growth [3], and spontaneous mutations [4]) and rare dissipation events that are instantaneous on the time scale of driving (e.g., sand avalanches, earthquakes, fires, or a series of rapid mutations). In the stationary state, the size distribution of dissipation events obeys a power law, irrespective of initial conditions and without the need to fine-tune parameters. There is, however, no reason to expect that systems with slow driving and instantaneous avalanches always show SOC. Such systems might also have many small avalanches that release only little energy, or only large avalanches that release a finite part of the system's energy, or some combination of both. SOC systems are naturally at the critical point due to e.g., a conservation law (sandpile model), a second time scale separation (forest-fire model), a competition between open boundary conditions and the tendency of neighboring sites to synchronize (earthquake model [2,5]; see, however, [6] for a counterexample), or extremal dynamics (''evolution'' model [4]). Often, the critical behavior breaks down when details of the model rules are changed (e.g., the boundary conditions in the earthquake model [5] or the tree growth rule in the forest-fire model [7]).

There are certain parallels between these models and equilibrium critical systems since both consist of many small units that interact with their neighbors and spin clusters in an Ising model or clusters of occupied sites in percolation theory can be compared to avalanches. However, the critical behavior of nonequilibrium systems can depend on microscopic details, as mentioned above, in contrast to equilibrium critical phenomena, which commonly show universal behavior. Also, nonequilibrium systems do not satisfy a detailed-balance condition and can, e.g., show periodic behavior. Furthermore, avalanches are usually released when some variable reaches locally a threshold while other regions of the system might be far below the threshold, and consequently not all parts of the system look equal. This can in particular result in more than one diverging length scale, as in the earthquake model [5] or in the forest-fire model [8]. By contrast, in equilibrium systems the energy is an extensive variable, which means that all regions (which are large compared to the lattice constant) are equal. This is, e.g., the basis for hyperscaling relations.

In this paper, we discuss in detail a model [9] that belongs to the mentioned class of nonequilibrium systems with avalanchelike dynamics. It is a nonequilibrium percolation model, where clusters of occupied sites are removed and the same number of sites that have become empty are occupied at random. The density of occupied sites is the control parameter of the model. The ''avalanches'' of our model are removal events and the size of an avalanche is the size of a removed cluster. This model illustrates well the fundamental differences between equilibrium and nonequilibrium, showing various features that are not observed in equilibrium systems: The region of small avalanches and the region of infinite avalanches are separated by a finite region of critical behavior, where the correlation length diverges more slowly than the system size. The exponent that relates the system size with the correlation length depends on the density. Besides the correlation length, there are other relevant length scales. Since the critical behavior occurs over a finite density interval, the system can exhibit power laws naturally, without fine-tuning of parameters to a precise value. Therefore, our model belongs to the class of SOC systems. In the region of infinite avalanches, the system shows synchronization with a period that depends on the value of the density. We illustrate and explain all these observations using computer simulations and analytical arguments. Part of the results were already published in [9].

The work is structured as follows. In Sec. II, we define the model. In Sec. III, the subcritical phase and the critical point of the model are treated. The mechanism that leads to criticality and the value of the critical density are explained and the exponent of the cluster size distribution in one dimension is calculated analytically. Section IV discusses the critical phase. The reason for the existence of a whole critical phase as well as for its properties such as nonstandard finite-size scaling and violation of hyperscaling are explained. The supercritical phase is treated in Sec. V. First, we explain the

existence of synchronized stripes and their relation to the subcritical phase (Sec. V A), then we discuss hysteresis and the maximum possible number of stripes (Sec. V B), and, finally, we investigate stability, movement, and roughness of stripes (Sec. V C). In Sec. VI, we summarize and discuss our work.

II. DEFINITION OF THE MODEL

The nonequilibrium percolation model is defined on a d-dimensional hypercubic lattice with L^d sites. Each site is either occupied or empty. The control parameter of the system is the density of occupied sites ρ.

The dynamics are defined by the following rules. (i) An occupied site in the system is chosen at random and the whole cluster of s occupied sites connected to this site (by nearest-neighbor coupling) is removed from the system, i.e., the occupied sites of that cluster turn to empty sites. (ii) We occupy s randomly chosen empty sites (possibly also including sites that have become empty due to the removal of the cluster). (iii) Proceed with (i).

These rules ensure that the density of occupied sites ρ is a conserved quantity. Starting with a random initial state, the system approaches after a transient time a stationary state that is characterized by a certain size distribution of clusters where the time average and ensemble average of all quantities are identical. Throughout this paper, we discuss only the properties of the stationary state. These properties, which are explained in detail Secs. III–V, are as follows. For small densities, there are only small clusters of occupied sites in the system. With increasing density, the size of the largest cluster increases, and it diverges at a critical density ρ_c. For $\rho_c<\rho<\rho_c^{(2)}$, the system is critical, i.e. the cluster size distribution is a power law. The size of the largest cluster diverges more slowly than the system size. For $\rho>\rho_c^{(2)}$, the system has a finite number of regions of different density. The region with the highest density has a spanning cluster.

One can think of the dynamics of this model as ''explosions'' that take place at a randomly chosen site. During the explosion, the whole cluster connected to the explosion site is blown up and its constituents settle down somewhere else in the system. Alternatively, one might think of colonies of animals that are dispersed into all directions by some enemy or other event. From a more abstract point of view, one has a nonequilibrium percolation problem.

This model is also closely related to the self-organized critical forest-fire model (FFM) [3] when occupied sites are equated with trees: For $\rho<\rho_c$, the correlation length ξ and the mean number of removed sites per step S are finite and all properties of the stationary state can be found by looking at a section of the system of linear size ℓ, with $\xi<\ell\ll L$. In this section, there is no conservation of density and the dynamics can be characterized by a small ''tree growth'' rate $p=S\rho(\ell/L)^d/(1-\rho)$ and a ''lightning'' rate $f=(\ell/L)^d$. The tree growth rate is the probability that a given empty site becomes occupied during one step and the lightning rate is the probability that a given site is ''struck by lightning'' (i.e., selected) per step, with the consequence that all ''trees'' connected to this site ''burn down'' (i.e., are removed). S diverges in the limit $f/p\to 0$ as

$$S=p(1-\rho)/f\rho. \tag{1}$$

In this limit, ρ approaches the critical value ρ_c. The dynamics in the small region of size l are the same as for the SOC FFMI; and the critical exponents close to ρ_c are therefore the same as those of the SOC FFM in the limit $f/p\to 0$, when the f/p dependence is translated properly into a ρ dependence (simulation results of the SOC FFM can be found in, e.g., [10–13,8]). Choosing ρ as the control parameter instead of f/p allows us to study the FFM beyond the critical point. This was in fact our original motivation to introduce the model studied in this paper.

In the following three sections, we discuss in detail the subcritical, the critical, and the supercritical behavior of the model. Unless stated otherwise, the considered system is a two-dimensional square lattice.

III. SUBCRITICAL PHASE AND APPROACH TO THE CRITICAL POINT

First, we discuss the parameter region $\rho<\rho_c$, where the system has a cutoff in cluster size that is independent of the system size L. Let S be the mean number of sites removed from the system in one time step, without taking into account the refilling of sites. For very small densities, there exist only very small clusters and most clusters will consist of only one site. The process of removing clusters (in this case mostly single sites) and refilling sites at random does not change this situation, i.e., S is of the order of one, and the occupied sites remain randomly distributed, as for a percolation system at small densities.

With increasing density, S increases also. Removing the chosen cluster and refilling its sites at random into the system introduces fluctuations in the local density of occupied sites because the removed cluster leaves behind a ''hole'' and the refilled sites increase the density in the rest of the system to a value larger than ρ. The critical density ρ_c, where S diverges, and the critical exponents close to ρ_c are therefore different from their values in percolation theory.

We define the usual quantities that are investigated in percolation systems (for an introduction to percolation, see [14]): The number density of clusters of occupied sites of size s will be denoted by $n(s)$. Near a critical density ρ_c, $n(s)$ is expected to behave like a power law

$$n(s)\propto s^{-\tau}\mathcal{C}(s/s_{\max}), \tag{2}$$

where $\mathcal{C}$ is a scaling function and $s_{\max}\propto|\rho_c-\rho|^{-1/\sigma}$. The average cluster size S is defined by

$$S=\frac{\sum_{s=1}^{\infty} s^2 n(s)}{\sum_{s=1}^{\infty} s n(s)} \tag{3}$$

and is expected to diverge like

$$S\propto|\rho_c-\rho|^{-\gamma}. \tag{4}$$

The correlation length ξ is defined as the root-mean-square distance between occupied sites on the same cluster, averaged over all clusters, which leads to

$$\xi^2 = \frac{\sum_{s=1}^{\infty} R^2(s) s^2 n(s)}{\sum_{s=1}^{\infty} s^2 n(s)}. \tag{5}$$

Near a critical point, ξ is expected to diverge like

$$\xi \propto |\rho_c - \rho|^{-\nu}. \tag{6}$$

The radius of gyration R of a cluster grows with its size s like

$$R(s) \propto s^{1/d_f}, \tag{7}$$

with the fractal dimension d_f. These critical exponents are related via the scaling relations $1/\sigma = \gamma/(3-\tau) = d_f \nu$. Finally, the strength of an infinite cluster is denoted by P. In percolation, P follows a power law

$$P \propto (\rho - \rho_c)^{\beta}$$

above the critical point.

In our simulations, we found $\rho_c \simeq 40.8\%$, $\tau = 2.15(3)$, $d_f = 1.96(2)$, $\nu = 1.20(5)$, and $\gamma = 2.09(5)$. The values of these exponents as well as the value of the critical density ρ_c are different from percolation theory, and they are identical with the corresponding values of the SOC FFM. The $\rho_c - \rho$ dependence of our model can be translated into the f/p dependence of the FFM using Eqs. (4) and (1), giving

$$\rho_c - \rho \propto (f/p)^{1/\gamma}.$$

Thus our values of σ and ν can be calculated from those of the FFM by multiplication with γ. τ and d_f are exponents related to the cluster size s, so no multiplication with γ is necessary. The exponent β vanishes, as we shall see in Sec. IV.

The above-mentioned fluctuations in the local density of occupied sites can easily be seen by looking at a snapshot of the system for densities close enough to the critical density. A typical stationary state for the density $\rho = 39.3\%$ and system size $L = 1024$ is shown in Fig. 1. One can see that the system consists of a large number of regions with different and rather homogeneous density. The typical size of these ''patches'' does not depend on the system size L, provided that L is large enough. Many properties of the model can be understood by describing the system in terms of these patches of homogeneous density of occupied sites. For small average patch size (like in Fig. 1), it is not always possible to assign a given site unequivocally to a certain patch. This changes, however, when the critical density is approached, where the mean patch size is larger and the patch boundaries become sharper.

For large system size $L^2 \gg S$, only a few sites are occupied in a given patch per time step and the density $\rho(t)$ in a patch evolves continuously according to $\rho'(t) = p[1-\rho(t)]$ with some growth rate p, which leads to

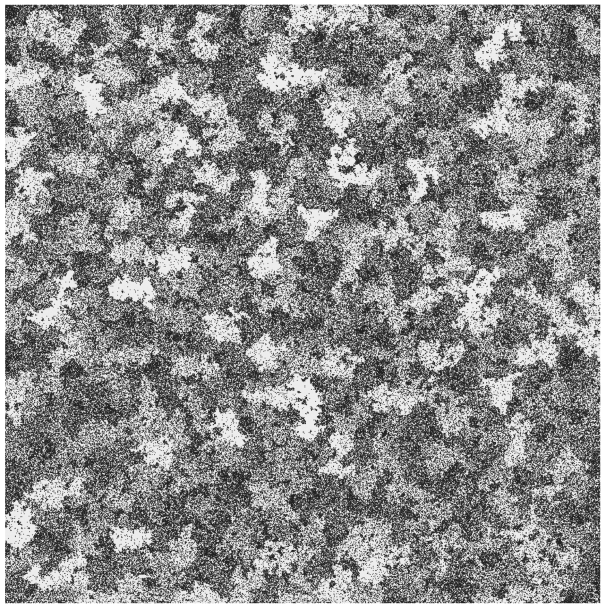

FIG. 1. Stationary state at $\rho = 39.3\%$ and $L = 1024$ (with periodic boundary conditions, square lattice with nearest neighbors, occupied sites are black, and empty sites are white).

$$\rho(t) = 1 - (1-\rho^{\text{after}}) \exp(-pt). \tag{8}$$

Here time is measured since the removal event that produced that patch, leaving behind a small density of occupied sites $\rho(0) \equiv \rho^{\text{after}}$. We also define the mean density ρ^{before} of a patch just before its spanning cluster is removed and the time T that it takes to increase the density from ρ^{after} to ρ^{before}. We easily derive $T = (1/p) \ln[(1-\rho^{\text{after}})/(1-\rho^{\text{before}})]$. The average density of a patch is

$$\rho = \frac{1}{T} \int_0^T dt [1 - (1-\rho^{\text{after}}) e^{-pt}] = 1 - \frac{\rho^{\text{before}} - \rho^{\text{after}}}{\ln\left(\frac{1-\rho^{\text{after}}}{1-\rho^{\text{before}}} \right)}. \tag{9}$$

We measured the average values $\rho^{\text{before}} \approx 62.5\%$ and $\rho^{\text{after}} \approx 7.8\%$, similar to the values found in [15,8]. Interestingly, the same values will play an important role in the critical phase and in the striped phase discussed in Secs. IV and V. With the measured values of ρ^{before} and ρ^{after}, we obtain as average density of one region $\rho = 39.2\%$. For large enough system size L^2 and neglecting the interactions between the different regions, the time average of the overall density ρ would also be $\rho = 39.2\%$. In a real system with interacting regions, the mean density is in general different due to the following two mechanisms. (i) There are temporal oscillations in patch size: During the growth process of the density of a patch from ρ^{after} to ρ^{before}, all the neighboring patches have one removal process on an average. During each of those removals, also some sites of the central patch are removed because patch boundaries are not cluster boundaries. This leads to a shrinking of the area of the original patch while its density increases, reducing the mean density from the above calculated value. (Of course, the original patch size is ultimately restored when the spanning cluster of the central patch and some finite clusters of neighboring patches are finally removed.) The relative shrinking of the

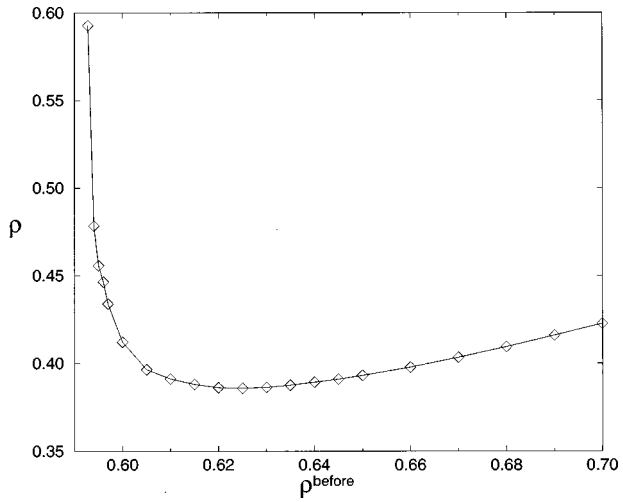

FIG. 2. Average density ρ for various values of ρ^{before} between 59.3% and 70%. The minimum is at approximately 62.5.

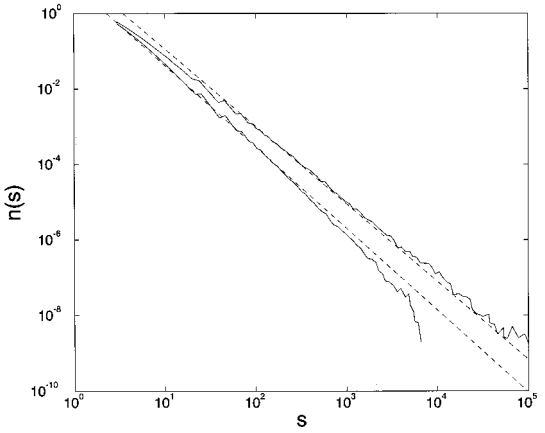

FIG. 3. Upper curve; cluster size distribution $n(s)$ of a homogeneous system at the percolation threshold $p_c \approx 59.3\%$; lower curve; cluster size distribution $n(s)$ of a system with densities between ρ^{after} and ρ^{before}, distributed according to Eq. (8). Both systems have size $L=2048$. The dashed straight lines have slope 2.06 and 2.15, respectively.

area is stronger for smaller mean size of removed patches since the number of sites removed from the central patch depends on the length of its boundary. For large mean size of removed patches, the ratio of the initial patch size to the final patch size approaches 1, i.e., $\rho = 39.2\%$, which explains why the density is smaller than the critical density when the mean size of removed patches (of the order S) is finite. (Fluctuations in the size of removed patches are complicated to consider and do not affect our main conclusions.) (ii) The critical density itself is larger than the above value $\rho = 39.2\%$ because the density at which a removal event takes place fluctuates around its mean value ρ^{before}. Assuming a homogeneous distribution of occupied sites within a region, we measured the mean density ρ for various densities ρ^{before} between 59.3% and 70%. The result is shown in Fig. 2. One can see that this function has a minimum for the measured average value of $\rho^{\text{before}} \approx 62.5\%$. Any fluctuation will therefore lead to an increase in the mean value of ρ. The fact that the density is so close to its minimum indicates a tendency of the system to maximize energy dissipation. To obtain the order of magnitude of the shift in ρ_c due to fluctuations, we calculated numerically the mean density in the simulated interval $[p_c; 0.70]$ of ρ^{before}. The result is 40.5(3)%, which is close to the correct critical density $\rho_c \simeq 40.8\%$, indicating that the fluctuations in ρ^{before} can indeed induce the observed shift in the density.

These considerations show that the critical state of our model can, to a good approximation, be interpreted as a combination of percolation systems of different densities, as also suggested in [8]. The cluster size distribution $n(s)$ is therefore the superposition of the cluster size distributions of all the patches with their different densities between ρ^{after} and ρ^{before}, distributed according to Eq. (8).

Let us first consider the one-dimensional system. There the percolation threshold is one and even in dense regions all clusters are finite percolation clusters. Removal of a cluster leaves behind a string of empty sites. The system is therefore composed of strings of size S of different densities that represent different stages in the growth process of an empty string until it is completely filled. A string of density ρ contains a cluster of size s with probability $\rho^s(1-\rho)^2$. If the system size L is large enough, the time average equals the ensemble average and the cluster size distribution should be given by

$$
\begin{aligned}
n(s) &\propto \int_0^\infty dt \rho(t)^s [1-\rho(t)]^2 = \int_0^\infty dt (1-e^{-pt})^s (e^{-pt})^2 \\
&\propto \int_0^\infty dt \sum_{k=0}^{s} \binom{s}{k} (-1)^k e^{-kt} e^{-2t} \\
&= \sum_{k=0}^{s} \binom{s}{k} (-1)^k \frac{1}{2+k} = \frac{1}{(s+1)(s+2)} \\
&\approx s^{-2} \text{for large } s,
\end{aligned}
$$

in agreement with the exact calculation of [16]. Similarly, the size distribution of hole clusters is found to be

$$
\begin{aligned}
h(s) \int_0^\infty dt \rho(t)^2 [1-\rho(t)]^s &\propto \frac{1}{s(s+1)(s+2)} \\
&\approx s^{-3} \text{for large } s,
\end{aligned}
$$

again in agreement with exact results [17,16].

For dimensions higher than one, unfortunately, these calculations cannot be carried out. There the number of neighbors t of a cluster of size s depends not only on s, but also on the shape of the cluster, and the number of different clusters with a given size s and a given perimeter t is not known exactly. Furthermore, the integration over t does not go from zero to infinity since the lowest and highest densities are not 0 and 1, respectively. We can, however, determine numerically the cluster size distribution of a combination of percolation systems of different densities. We measured $n(s)$ in 20 homogeneous systems with $L=2048$ and different densities between ρ^{after} and ρ^{before}, distributed according to Eq. (8). The total $n(s)$ of all systems proportional to $\Sigma_{i=1}^{20} n_i(s)$ is plotted in Fig. 3, together with the cluster size distribution of a percolation system at $\rho = p_c \approx 0.593$. The exponent

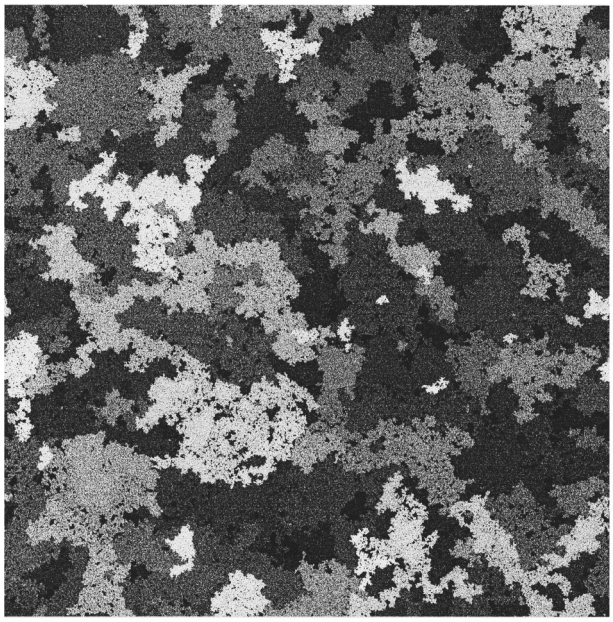

FIG. 4. Stationary state at the critical density $\rho_c \approx 40.8\%$ and $L=4096$ (with periodic boundary conditions, square lattice with nearest neighbors, occupied sites are black, and empty sites are white).

$\tau \approx 2.15$ for a combination of percolation systems is indistinguishable from the cluster size distribution exponent of our model, showing that the latter is indeed generated by a superposition of percolation systems. Figure 3 does not show the bump observed in our simulations for large s. For large cluster sizes, the size distribution of patches with density above the percolation threshold affects the cluster size distribution. This effect is not present in Fig. 3, where there are no different patch sizes. It remains an open question whether the exponent τ remains the same for much larger values of s than those accessible to simulations. At very large scales, the emerging dynamics of patches might become an important factor in determining the cluster size distribution.

Another conclusion that can be drawn is that τ always has to be larger than or equal to the τ of the corresponding percolation problem. $n(s)$ results from a superposition of many percolation systems, so that apart from the critical percolation system, there exist also many systems with finite cutoff in the cluster size distribution. These systems increase the weight of the small clusters and the slope of $n(s)$ decreases, resulting in a larger τ. For all dimensions and lattice types investigated so far (see, for example, [13]), this was true.

IV. THE CRITICAL PHASE, HYPERSCALING, AND FINITE-SIZE SCALING

For $\rho > \rho_c$, one might expect the appearance of an infinite cluster that spans the whole system, as in percolation theory. However, the values of the critical exponents for $\rho \lesssim \rho_c$ already indicate that the situation in our system is very different from percolation. In contrast to percolation, the hyperscaling relation $d = d_f(\tau - 1)$ is violated, which means that not every part of the system contains a spanning cluster at criticality [10]. This can also be seen easily by looking at the snapshot of a system at $\rho \approx \rho_c$ in Fig. 4. In addition to large patches with high density, there exist also large patches with lower densities. Most of the patches have densities below the percolation threshold and contain many finite clusters. The patches with high densities (between p_c and $\approx 62.5\%$) contain not only finite, but also ''infinite'' (i.e., spanning) clusters. In contrast to ordinary percolation, there is no homogeneously distributed set of large clusters that could join at $\rho = \rho_c$ to form the infinite cluster that spans the whole system. Rather, besides the largest cluster, the system contains many other large clusters that represent different growth stages of the largest cluster itself. The critical behavior of our model occurs over a finite interval $[\rho_c^{(1)} (= \rho_c \approx 40.8\%), \rho_c^{(2)} (\approx 43.5\%)]$, where the cutoff in cluster size $s_{\max}$ diverges, but more slowly than L^2. The correlation length diverges more slowly than L. Since it is not possible to define a truly infinite cluster like in percolation in this phase, all clusters in the system contribute to the defining equations of $s_{\max}$, ξ, and S. We find

$$s_{\max} \propto L^{\phi_1}, \quad \xi \propto L^{\phi_2}, \quad S \propto L^{\phi_3},$$

with ρ-dependent exponents $\phi_{1,2,3}$, while τ and d_f remain unchanged. Table I shows the values of the exponents for different densities. Figure 5 shows a snapshot of the system for $\rho = 0.43$.

TABLE I. Exponents $\phi_{1,2,3}$ of $s_{\max}$, ξ, and S for various densities $\rho_c^{(1)} < \rho < \rho_c^{(2)}$ ($L = 512, 1024, 2048, 4096$)

ρ	ϕ_1	ϕ_2	ϕ_3
0.41	1.46(8)	0.79(2)	1.23(3)
0.42	1.72(6)	0.92(3)	1.50(3)
0.43	1.86(8)	0.97(3)	1.62(3)
0.435	1.92(8)	0.99(2)	1.69(5)

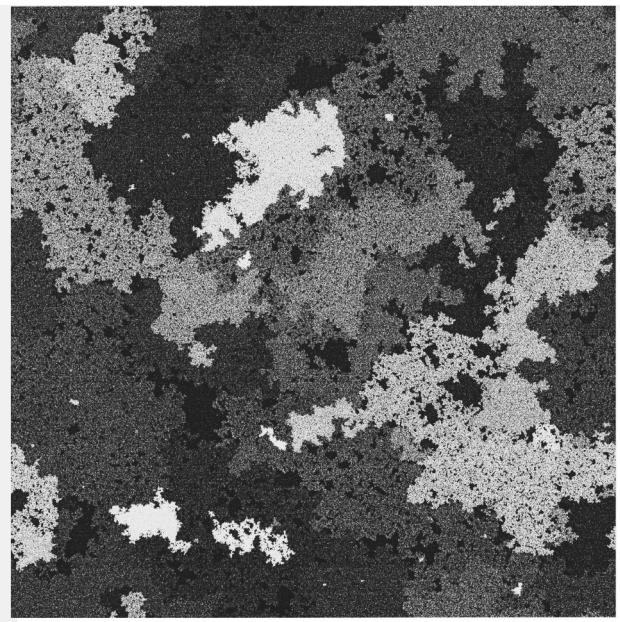

FIG. 5. Stationary state at $\rho = 43\%$ and $L = 4096$ (with periodic boundary conditions, square lattice with nearest neighbors, occupied sites are black, and empty sites are white).

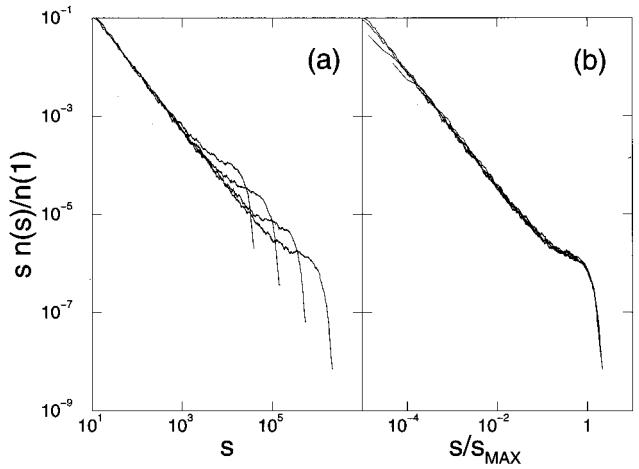

FIG. 6. Normalized size distribution of clusters for $\rho=0.43$ and $L=512,1024,2048,4096$, (a) before and (b) after rescaling.

Figure 6 shows the size distribution of clusters $sn(s)$ for different system sizes at fixed ρ (a) before and (b) after rescaling. With Eqs. (2) – (7) one can derive the scaling relations $\phi_1=d_f\phi_2$ and $\phi_3=(3-\tau)\phi_1$, which are well confirmed by the simulations. For $\rho\to\rho_c^{(2)}$, $\phi_{1,2,3}$ approach the values d_f, 1, and $1/\nu$, respectively.

The latter values are those that one would already have expected at $\rho=\rho_c^{(1)}$ from finite-size scaling theory. In a critical system, a quantity X that scales as $|T-T_c|^{-\chi}\propto\xi^{\chi/\nu}$ in an infinite system, in a finite system is expected to obey the scaling form

$$X(L,\xi)=\xi^{\chi/\nu}\hat{X}(\xi/L),$$

with

$$\hat{X}(x)=\begin{cases}\text{const} & \text{for } x\ll 1\\ x^{-\chi/\nu} & \text{for } x\gg 1\end{cases}$$

such that for $\xi\ll L$, $X\propto|T-T_c|^{-\chi}$, like in the infinite system, and for $L\ll\xi$, $X\propto L^{\chi/\nu}$. The standard finite-size scaling exponents of $s_{\max}$, ξ and S would therefore be $1/\nu\sigma=d_f$, $\nu/\nu=1$, and $1/\nu$.

The main difference between our system and percolation concerning finite-size scaling is that in percolation a system of length L_{large} without finite-size effects can be generated by putting together systems with finite-size effects of length L_{small}. In our model, a reorganization takes place when smaller systems are put together since the smaller systems now can have fluctuations in their number of occupied sites that they could not have when they were isolated. Due to the inhomogeneous nature of the stationary state, these fluctuations are very large.

We obtain a deeper understanding of the critical behavior of our model when we describe the system again in terms of patches of different densities. In Sec. III, we found that the density within a patch grows continuously for $\rho<\rho_c$ and for sufficiently large system size. For not sufficiently large system size and for $\rho>\rho_c$, however, the finite system size leads to discontinuous jumps in the density within a patch. The noncontinuous version of Eq. (9) is [see Eq. (13) below]

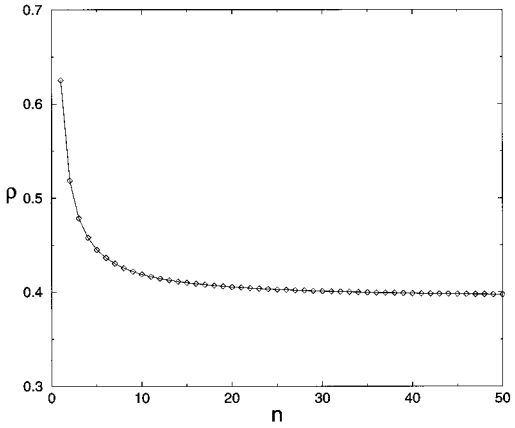

FIG. 7. ρ as function of the number of patches n with densities between ρ^{after} and ρ^{before}.

$$\rho=1-\frac{\rho^{\text{before}}-\rho^{\text{after}}}{n\{[(1-\rho^{\text{before}})/(1-\rho^{\text{after}})]^{-1/n}-1\}}$$

for the density of a system that takes n time steps to go from ρ^{after} to ρ^{before}. In Fig. 7, ρ is plotted as a function of the number of patches n. One can see that a decrease in n raises the mean density. (Of course, this conclusion can also be obtained from an analytical calculation.) This effect supplements the two other mechanisms that affect the mean density presented in Sec. III. For fixed ρ and changing L, these three mechanisms have to be in balance with each other. While the step size decreases with increasing L, tending to decrease the density, the size of the large patches and the fluctuations in ρ^{before} increase, canceling the effect of the smaller step size on the density.

So far, we have not yet discussed the possibility of fusion and splitting of patches. As soon as two neighboring patches have a density above the percolation threshold, they fuse and will be removed together. This effect must be balanced by a mechanism that splits patches. As long as the density of a patch is below the percolation threshold, neighboring removals move the boundary of this patch inward and a splitting into two patches occurs when opposite boundaries meet. A splitting can also occur when a finite cluster connecting two opposite edges of the patch is removed before the density in the patch reaches the percolation threshold. Since even large patches must split at the same rate at which they fuse with neighboring patches, the shape of patches cannot be round, but must be ''fingered,'' with necks of a width that does not depend on the patch size. The snapshots Figs. 4 and 5 show the fingered structure. It implies some characteristic length scale, the ''finger thickness,'' in addition to the lattice constant and the correlation length. This scale is a function of the density and the system size. The existence of several length scales was also observed in [8].

V. SUPERCRITICAL PHASE

A. Synchronized states

At $\rho=\rho_c^{(2)}$, the correlation length finally becomes proportional to the system size and the system has an ''infinite'' cluster that contains a finite percentage (independent of L) of

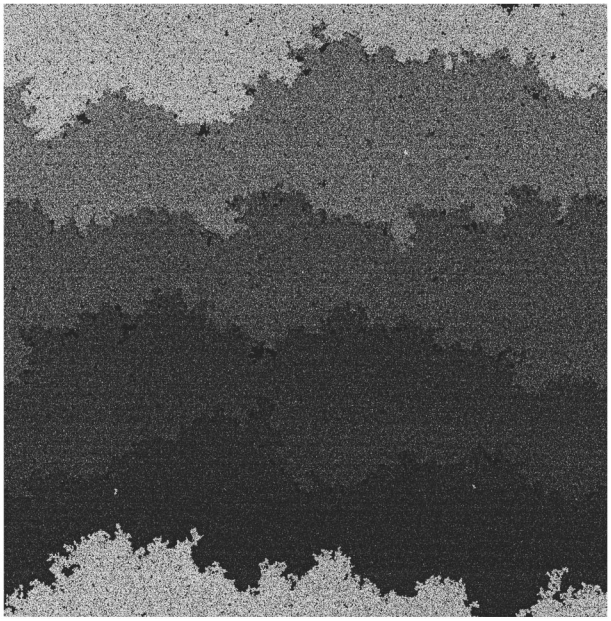

FIG. 8. Stationary state with five stripes at $\rho = 0.45$ and $L = 4096$ (with periodic boundary conditions, square lattice with nearest neighbors, occupied sites are black, and empty sites are white).

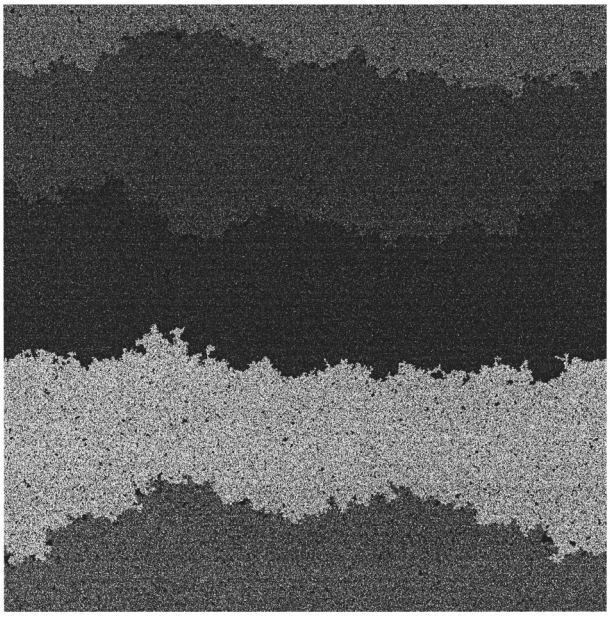

FIG. 9. Stationary state with four stripes at $\rho = 0.46$ and $L = 4096$ (with periodic boundary conditions, square lattice with nearest neighbors, occupied sites are black, and empty sites are white).

all occupied sites in the system. Figure 8 shows a snapshot of the system for $\rho = 0.45$. We see a system with five homogeneous and equally large stripes with different densities. The stripe with highest density is above the percolation threshold and contains an infinite cluster (with nonzero strength P) as well as some small clusters. The other stripes are below the percolation threshold and, consequently, contain only small clusters. When one of the small clusters in this state is removed, only a few sites are redistributed and the state of the system remains essentially unchanged. When the infinite cluster is removed, a large portion of all occupied sites in the stripe with the highest density are redistributed all over the system. The stripe that used to have the highest density now has the lowest density, while the density of the other stripes has increased. The values of the five densities are the same as before, except that they are now associated with different stripes. If we measure time in units of large redistributions of sites, the state of the system is periodic with period 5.

Increasing ρ, we find four stripes (Fig. 9), three stripes (Fig. 10), two stripes (Fig. 11), and finally one ''stripe'' (Fig. 12), where the infinite cluster spans the whole system. The spatial shape of stripes depends on lattice symmetry and boundary conditions. In the case of a two-dimensional square or triangular lattice with periodic boundary conditions, the system self-organizes into stripes with the boundaries along one of the principal axes. For absorbing boundary conditions, the stripes are replaced by regions of a different shape (see Fig. 10).

To understand the occurrence of stripes with different densities, we consider first a system with a very high density $\rho \lesssim 1$. Since we are far above the percolation threshold $p_c \approx 0.593$ for random site percolation, the strength of the infinite cluster P is close to ρ. We start with a random initial state. In the first iteration step, we remove either the infinite cluster, which consists of nearly all occupied sites in the system, or one of the finite clusters, which, consequently, are very small. In the first case, only a few small clusters remain and most of the occupied sites are redistributed randomly in the system. In the second case, only a small number of occupied sites are redistributed. In both cases, however, the state of the system changes little and the new state is close to a completely random state.

If we now decrease ρ, the remaining clusters (after the removal of the infinite cluster) become larger and the density

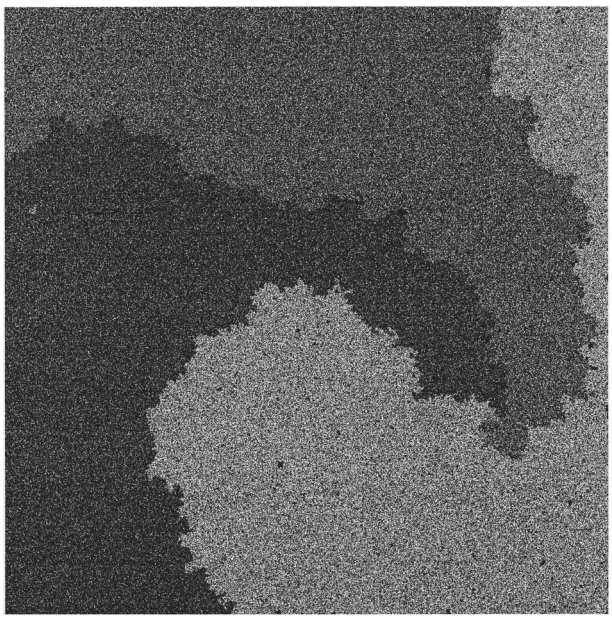

FIG. 10. Stationary state with three regions of different density at $\rho = 0.50$ and $L = 2048$ (with absorbing boundary conditions, square lattice with nearest neighbors, occupied sites are black, and empty sites are white).

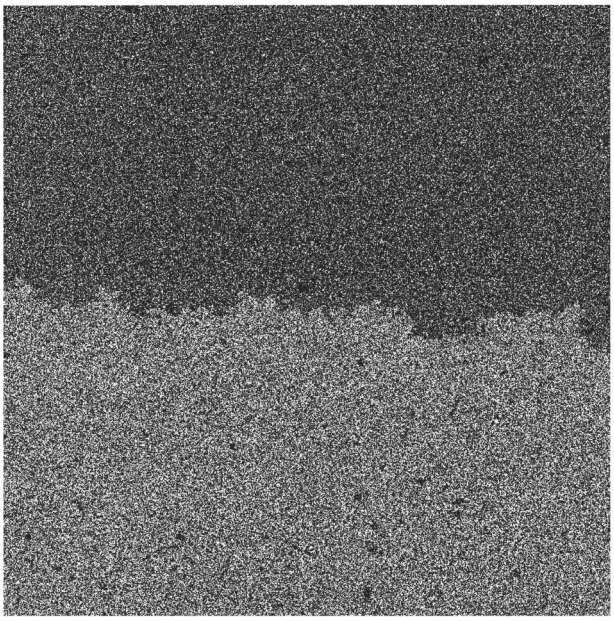

FIG. 11. Stationary state with two stripes at $\rho = 0.55$ and $L = 1024$ (with absorbing boundary conditions, square lattice with nearest neighbors, occupied sites are black, and empty sites are white).

fluctuations increase. When the removed sites are refilled into the system, part of them are positioned in or near these surviving clusters, where the density then will be larger than the mean density. In the space between these clusters the density consequently is lower than the mean density (see Fig. 13). If ρ falls below a certain threshold ρ^*, this density between the surviving clusters becomes smaller than the percolation threshold p_c. Then, there exists no infinite cluster in the system after the first time step (or after a few iterations)

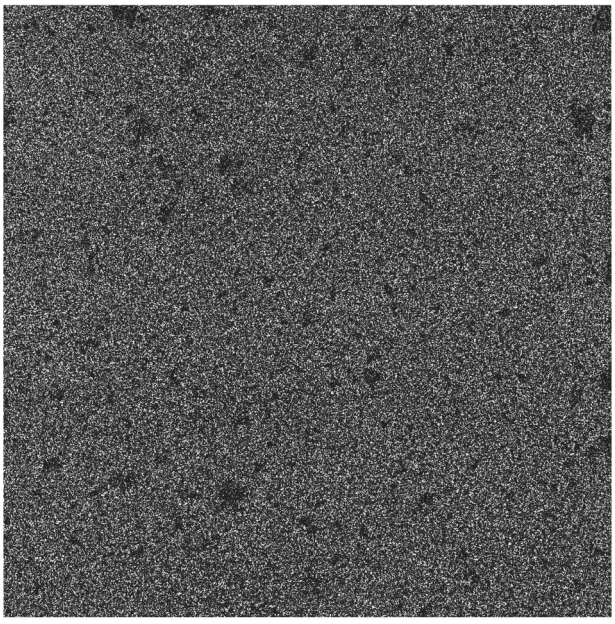

FIG. 12. Stationary state at $\rho = 0.63$ and $L = 1024$ (with absorbing boundary conditions, square lattice with nearest neighbors, occupied sites are black, and empty sites are white).

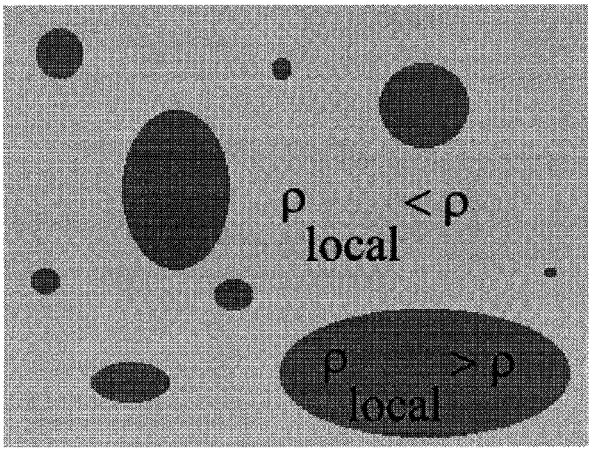

FIG. 13. Schematic picture of the stationary state at a density just above ρ^*. Light (dark) gray regions have lower (higher) than average density.

and the state with one stripe becomes unstable. Evidently, $\rho^* > p_c$.

The approximate value of ρ^* can be derived by the following argument. The number of empty sites after the removal of the infinite cluster is $L^2[1-(\rho-P)]$. Let this subset of the total lattice be denoted by $\mathcal{D}$. It contains the area of the infinite cluster and the sites that have already been empty before. In the next step, the L^2P occupied sites of the infinite cluster are redistributed randomly among these empty sites, leading to a density $\rho' = P/[1-(\rho-P)] < \rho$ in $\mathcal{D}$. In the vicinity of the clusters that were left over the local density is now higher than before. One can think of this state approximately as consisting of many compact clusters embedded into a lower-density background (see also Fig. 13). It is then obvious that the homogeneous state with an infinite cluster stretching over the whole system cannot survive if $\rho' < p_c$, since, in this case, the infinite network that links the finite high-density regions is broken. On the other hand, if $\rho' > p_c$, the situation is not fundamentally different from the case $\rho \lesssim 1$. Fluctuations in the local density do exist, but they cannot get stronger with time since the high-density regions are themselves removed from the system with high probability during the next few iteration steps. Thus we arrive at the implicit approximate equation for a threshold density ρ^*,

$$\frac{P(\rho=\rho^*)}{1-\rho^*} = \frac{p_c}{1-p_c}. \tag{10}$$

In the simulations, we found $\rho^* \approx 0.625$ for the square and 0.533 for the triangular lattice. A measurement of the left-hand side of Eq. (10) at $\rho = \rho^*$ and $L = 1024$ yielded approximately 1.46 for the square and approximately 1.01 for the triangular lattice. The values of the known right-hand side are approximately 1.46 and 1, respectively. Although Eq. (10) is approximate, the agreement with simulation results is very good.

If ρ falls below ρ^*, the homogeneous phase becomes unstable and the system rearranges itself to a new stationary state that consists of two homogeneous stripes with equal area and different densities ρ_1 and ρ_2 ($\rho_1 > \rho_2$). For $\rho \lesssim \rho^*$, we have $\rho_1 > \rho^*$ and $\rho_2 < \rho^*$. When the infinite clus-

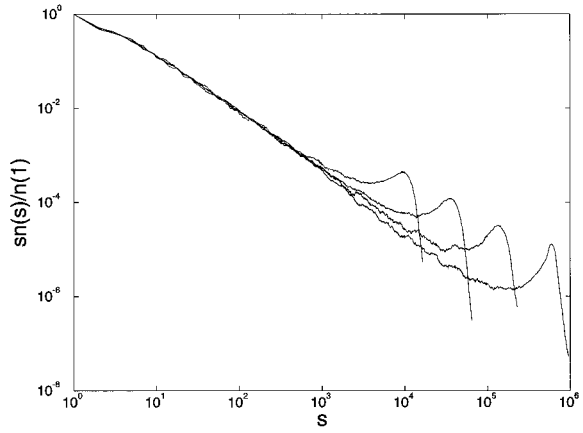

FIG. 14. Cluster size distribution of a system at $\rho=0.46$ for various system sizes ($L=512,1024,2048,4096$).

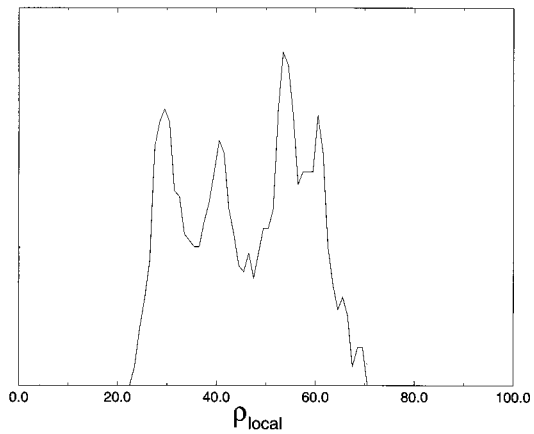

FIG. 15. Histogram of the local density ρ_{local} for $L=1024$ and $\rho=0.46$, averaged over 20^2 lattice sites.

ter in this new state is removed, the density of stripe 1 decreases to $\rho_3 \equiv \rho_1 - P$. Now these sites are reinjected randomly into the system, such that stripe 1 is filled up to ρ_2 and stripe 2 to ρ_1. The net effect is that the two stripes have changed their roles.

If we lower ρ further, we will eventually reach the density ρ for which $\rho_1=\rho^*$. At this point the two-stripe state becomes unstable (because the highest-density stripe becomes unstable) and reorganizes into a three-stripe state, thereby increasing ρ_1 such that $\rho_1>\rho^*$ again. The dynamics of the three-stripe state is analogous to the two-stripe state: When the infinite cluster is redistributed, the stripes simply exchange their densities ($3\rightarrow 2$, $2\rightarrow 1$, and $1\rightarrow 3$). With decreasing density, the number of stripes n increases further.

The stripe structure breaks down when the system size becomes so small that the width of a stripe is of the same order as the roughness of its boundary. The resulting state shows patches of different size, but differs from the critical state in its cluster size distribution. In Fig. 14, the cluster size distributions for a system at $\rho=0.46$ in the ''patched'' state ($L=512,1024$) and ''striped'' state ($L=2048,4096$) are plotted. The transition between the two seems continuous, due to finite-size effects. With increasing L, the bump becomes more distinct because the system tries to separate one infinite cluster from the ensemble of all clusters. There is no scaling of $n(s)$, not even in the ''patched'' states. With increasing system size, the bump should separate completely from the size distribution of finite clusters and move towards $s=\infty$. The distribution of densities in the system changes also continuously with increasing L when the transition from patches to stripes is made. Figure 15 shows a histogram of the local density for $L=1024$, i.e., for the patched state, averaged over 20^2 sites. This histogram shows pronounced peaks that are precursors of the stripes. In the limit of infinite system size, these peaks will become infinitely sharp.

The densities of the different stripes are related by several equations. Let $\rho_1,\ldots,\rho_n$ be the densities in a state with n stripes, starting with the highest density. Additionally, we define the density ρ_{n+1} of the stripe that contained the infinite cluster, immediately after the infinite cluster has been removed from the system and before the removed sites are refilled into the system. As a consequence of a large redistribution, the different stripes just exchange their densities, i.e.,

$$\rho_{i-1}=\rho_i+(\rho_1-\rho_{n+1})(1-\rho_i)/[n(1-\rho)+\rho_1-\rho_{n+1}] \tag{11}$$

for $i=2,\ldots,n+1$. The last factor on the right-hand side represents the fraction of occupied sites of the infinite cluster that are refilled in the stripe with density ρ_i. We finally obtain

$$\frac{1-\rho_1}{1-\rho_2}=\frac{1-\rho_2}{1-\rho_3}=\cdots=\frac{1-\rho_n}{1-\rho_{n+1}}. \tag{12}$$

Together with $\rho=(1/n)\Sigma_{i=1}{}^{n}\rho_i$ we have n equations for $n+1$ densities. The average density in a system with n stripes is then

$$\rho=1-\frac{1-\rho_{n+1}}{n}\sum_{i=1}^{n}\left(\frac{1-\rho_1}{1-\rho_{n+1}}\right)^{i/n}$$

$$=1-\frac{\rho_1-\rho_{n+1}}{n\{[(1-\rho_1)/(1-\rho_{n+1})]^{-1/n}-1\}}. \tag{13}$$

This equation was already used in Sec. IV.

The striped phase has several features in common with the critical and subcritical phase: They can all can be characterized by regions of different density. The density of these regions goes through a cycle and the spanning cluster of a region is removed when its density is of the order $\rho^*\approx 62.5\%$. Although there is no strict synchronization in the subcritical and critical phase, the system seems to maintain many features of the synchronized phase, albeit with more irregularities and fluctuations. If there were no regions with $\rho_{\text{local}}=\rho^*$, they would be generated by the same mechanism as in the synchronized phase. The resemblance to the synchronized phase is especially evident in the one-dimensional case. There the critical point can be interpreted as a synchronized state with $\rho^*=1$, $\rho^{\infty}=0$, and an infinite number of stripes.

From our understanding of the striped phase and its stability, we cannot rule out the existence of gaps, i.e., values of

the density for which no synchronized phase is stable. The following scenario could occur. When decreasing the density of an n-stripe state below the stability threshold, the new density in stripe 2 after the restructuring could be too large (i.e., greater than p_c) for the state to be stable. In this case, the new $(n+1)$-stripe state would be stable only after lowering the overall density a bit further until $\rho_2 < p_c$. The intermediate state would then have some irregular patched structure. However, in our simulations we could not observe this phenomenon.

B. Hysteresis and maximum number of stripes

Since the transition between states with different numbers of stripes is discontinuous, hysteresis effects are to be expected. When the overall density ρ is decreased adiabatically, a state becomes unstable when ρ_1 falls below $\rho^* \simeq 0.625$ and its number of stripes increases by one (thereby also increasing ρ_1). When ρ is increased adiabatically, however, there is no reason why the system should necessarily rearrange itself at $\rho_1 = \rho^*$. The stripe with the highest density can never become unstable since it only comes closer to the ideal case of $P(\rho_1) = \rho_1$, where it consists only of the infinite cluster. The reorganization from an $(n+1)$-stripe state to an n-stripe state is then triggered by the stripe with second highest density ρ_2. In the limit of infinite system size, it takes place when this stripe starts to contain an infinite cluster, i.e., when ρ_2 approaches the percolation threshold. As long as $\rho_2 < p_c$, even the largest cluster in stripe 2 is small compared to the infinite extent of one stripe and cannot have any effect on the dynamics. For finite system size, however, the reorganization takes place as soon as the ratio ξ_2 / D exceeds a certain critical value, where D is a measure for the linear extent of one synchronized region (as, e.g., the thickness of a stripe in the two-dimensional system with periodic boundary conditions). Therefore, the effect of hysteresis in a finite system is difficult to observe when the number of stripes n increases. Only for the transition from the two-stripe state to the homogeneous state could we identify a significant interval of hysteresis. The two-stripe state could be kept alive up to $\rho = 0.64$ for $L = 4096$.

In the following, we argue that there exists an upper limit to the number of stripes n even in an infinitely large system. When lowering ρ, the difference $\rho_1 - \rho_2$ decreases with each additional stripe. If the number of stripes n was not bounded from above, we would have $\rho_1 - \rho_2 \to 0$ and $\rho_1 \to \rho^*$. Such a state could only be stable if the maximum cluster size was finite in all stripes but stripe 1, which, in turn, could only be possible if the percolation threshold was identical to ρ^*. Since the distribution of occupied sites within a stripe is not completely random, the percolation threshold can be different from the threshold for conventional site percolation. We can find its value by simulating the density sequence $(\rho_n, \rho_{n-1}, \ldots, \rho_1)$ for a single stripe. We start with a stationary state with density ρ just above ρ^*. We remove the infinite cluster and fill the system again randomly and continually, and we measure the percentage of the largest cluster for two different system sizes. The results are shown in Table II. We see from Table II that an infinite cluster exists already for $\rho = 0.60$ since P is nonvanishing and does not decrease with increasing L. Furthermore, we measured the correlation length of the finite clusters in the interval $0.57 \leqslant \rho \leqslant 0.62$, which shows a pronounced peak around $\rho = 0.59$ for both $L = 512$ and $L = 1024$ (see Table II). These results show that the percolation threshold for stripes is very close (if not identical) to p_c for site percolation. Thus states with $\rho_2 > 0.59$ cannot exist, and there must exist a minimum density gap $\Delta\rho = \rho_1 - \rho_2$ and, consequently, a finite maximum number N of stripes. Equation (12) gives a maximum possible number of $n = 11(\pm 2)$ stripes and a corresponding minimum mean density $\rho = 42(\pm 0.3)\%$. In our simulations, due to finite system size, we could observe a maximum number of $n = 5$ stripes at $\rho = 0.45$ and $L = 4096$ (see Fig. 8). For other lattice types, the maximum number of stripes and the densities where the phase transitions take place are of course different. The realization of an infinite number of stripes (i.e., a front moving through a continuum) is possible with different rules, where the occupied sites of the chosen cluster are removed one by one and are put back into the system, before the next site is removed (see [18]).

TABLE II. Percentage P of the largest cluster and the correlation length ξ for different densities $\rho = 0.57, \ldots, 0.62$ with $L = 512$ and $L = 1024$

ρ	$P(L=512)$	$P(L=1024)$	$\xi(L=512)$	$\xi(L=1024)$
0.57			57	58
0.58			85	89
0.59			133	145
0.60	0.33	0.34	62	75
0.61	0.46	0.47	36	28
0.62	0.52	0.53	13	14

A schematic phase diagram of the system for all densities from 0 to 1 is shown in Fig. 16. Since a state with n stripes is only stable if the thickness of a stripe is much larger than ξ_2, the phase boundaries depend on the system size L for small L. They become vertical for large L and the values of ρ, where the phase transitions take place, are well defined. As one can also see in Fig. 16, the minimum density of the synchronized phase is smaller than the upper limit $\rho_c^{(2)}$ of the critical phase. Since the transition from patches to stripes is discontinuous, it shows also hysteresis.

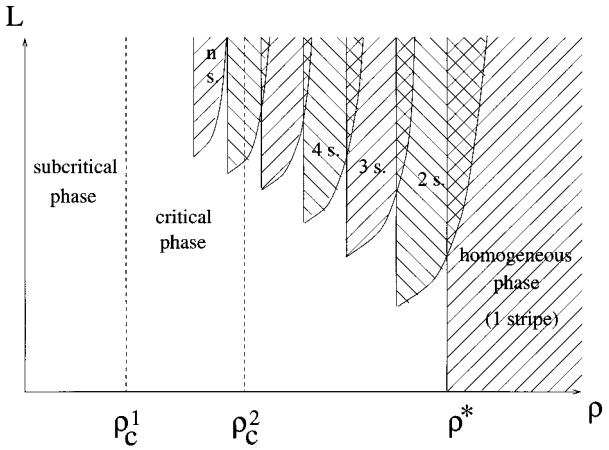

FIG. 16. Schematic phase diagram of a two-dimensional square system for all densities from 0 to 1.

C. Stability, movement, and roughness of stripes

In systems with $n>3$ stripes, there exists the possibility that the stripes might not be arranged in consecutive order with respect to their densities. However, these arrangements are not stable, as will be shown in the following. If the stripes are arranged in consecutive order, the stripe with highest density always has the same densities in its neighboring stripes during the complete cycle of length n. Each time the infinite cluster is removed, the borders of the stripe it has occupied expand ξ_2 to one side and ξ_n to the other. Since during one cycle the infinite cluster occupies each stripe position exactly once, all changes of width cancel. Since $\xi_2>\xi_n$, the whole pattern moves into the direction of the stripe with second highest density, as seen from the infinite cluster. If the stripes are not arranged in consecutive order, e.g. $\{\rho_1,\rho_3,\rho_2,\rho_4\}$, the changes in width do not cancel. The left neighbors of the infinite cluster during one cycle are $\rho_4,\rho_2,\rho_3,\rho_3$ and its right neighbors are $\rho_3,\rho_3,\rho_4,\rho_2$. Therefore, there is a net change of the width of some stripes on the expense of others and sooner or later (depending on system size) the structure breaks down and the system rearranges itself to a state with the stripes arranged in consecutive order. The instability of certain configurations like the one mentioned above was tested by starting with an artificially generated stationary state with the ''wrong'' order of stripes. After some time, the restructuring to the stable stationary state could be observed.

Similarly, if the area of different stripes is different or if the values of the stripe densities are not the same after each rearrangement of occupied sites, different stripes ''see'' a different environment when they are removed. Such states therefore cannot be stable. However, when they are close enough to the stable state, they return to it, as follows from the observed stability of striped states. In order to check explicitly the stability with respect to variations in the densities in a system with two stripes, we start with an unperturbed state at density ρ^0 with two stripes of density ρ_1^0 and ρ_2^0, respectively. The strength of the infinite cluster is $P^0=P(\rho_1^0)$ and $\rho_1^0-P^0=\rho_3^0$. Now we perturb the system by changing the densities to $\rho_1=\rho_1^0+\delta$ and $\rho_2=\rho_2^0-\delta$ with small $\delta>0$. The overall density ρ^0 is kept constant. The strength of the infinite cluster is now $P=P(\rho_1)=P(\rho_1^0+\delta)=P^0+\delta P'(\rho_1^0)$. After the removal of the infinite cluster the densities are $\rho_3=\rho_1-P=\rho_3^0-\delta(P'-1)$ and $\rho_2=\rho_2^0-\delta$. Using Eq. (11) one obtains for the highest density in the next iteration step

$$\rho_1^{\text{new}}=\rho_2^0-\delta+(P^0+\delta P')\frac{1-\rho_2^0+\delta}{2-(\rho_2^0+\rho_3^0)+\delta P'}.$$

TABLE III. Roughness exponent α, growth exponent β, and velocity v of the stripes for various densities ($200\leqslant L\leqslant 2000$).

ρ	No. of stripes	ρ^1	ρ^2	α	β	v
0.46	4	0.63	0.53			5.2(5)
0.50	3	0.66	0.51	0.44(10)	0.35(5)	4.3(5)
0.55	2	0.66	0.44	0.46(10)	0.25(5)	0

If this density is lower than the perturbed density $\rho_1=\rho_1^0+\delta$, the system tends to return to the unperturbed configuration and the initial state is stable. For stability, thus, the following inequality has to hold:

$$\rho_2^0-\delta+(P^0+\delta P')\frac{1-\rho_2^0+\delta}{2-(\rho_2^0+\rho_3^0)+\delta P'}$$

$$<\rho_2^0+P^0\frac{1-\rho_2^0}{2-(\rho_2^0+\rho_3^0)}+\delta.$$

On the right-hand side, we have used $\rho_1^0=\rho_2^0+P^0(1-\rho_2^0)/[2-(\rho_2^0+\rho_3^0)]$ from Eq. (11). This inequality can be rewritten as

$$P'<\frac{4(1-\rho^0)+3P^0}{\{1-P^0/[2(1-\rho^0+P^0)]\}(1-\rho_2^0)}. \tag{14}$$

We measured all quantities that appear in Eq. (14) in the density interval where the two-stripe state could be observed and found that it is completely contained in the interval where this condition is fulfilled.

As already mentioned above, the whole pattern of stripes moves into the direction of the stripe with second highest density seen from the infinite cluster. This movement can be observed in the simulations for all states with $n>2$. The net velocity in a two-stripe state is zero due to symmetry. We measured the velocity of this movement for stationary states with three and four stripes at $\rho=50\%$ and 46%. The results are $v\approx 4.3\pm 0.5$ lattice sites per iteration step for $\rho=50\%$ and $v\approx 5.2\pm 0.5$ for $\rho=46\%$. Since the degree to which the infinite cluster reaches into the neighboring stripes depends on their correlation lengths, the velocity is essentially determined by the density in stripe 2. As one can see from Table III, ρ_2 is larger for $\rho=46\%$ than for $\rho=50\%$, therefore the velocity is higher for $\rho=46\%$. The movement of the stripe boundaries can be seen in Fig. 17, where a sequence of stationary states of a three-stripe state is shown.

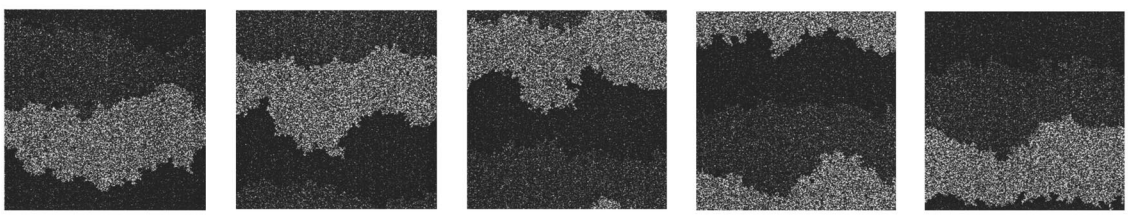

FIG. 17. Sequence of stationary states of a three-stripe state at $\rho=50\%$ and $L=1024$. The snapshots were taken at times t_0, t_0+51, t_0+102, t_0+153, and t_0+204.

As one can see in Fig. 8, the stripes seem to have rough rather than smooth boundaries. When the infinite cluster is removed, all finite clusters in the adjacent stripes that are connected to it are also removed. This leads not only to a net velocity in one preferred direction, but also to a roughening of the stripe boundaries, even in situations where the (artificially generated) initial state consists of strictly horizontal stripes.

The roughness of the interface is characterized by an exponent α that describes how the saturation width of the interface w_{sat} scales with its length L,

$$w_{\mathrm{sat}}(L) \propto L^{\alpha}.$$

The interface width w is defined as the root mean square of the differences $y(x)-\overline{y}(x)$, where $y(x)$ $[\overline{y}(x)]$ is the [averaged] y coordinate of the interface (assuming horizontal stripes)

$$w(L,t)=\sqrt{\frac{1}{L}\sum_{i=1}^{L}[y(x,t)-\overline{y}(t)]^2},$$

with $\overline{y}(t)=(1/L)\Sigma_{i=1}{}^{L}y(x,t)$. We assume that $y(t)$ is single valued, i.e., there are no overhangs. This assumption is always correct at sufficiently large scales.

To characterize the time-dependent dynamics of the roughening of the interface width $w(t)$, the growth exponent β is introduced by

$$w(L,t) \propto t^{\beta}.$$

For small t, there is no dependence on L since the information on system size needs a certain amount of time to spread. For an introduction to interface roughening, see [19].

We measured the roughness exponent α as well as the growth exponent β for stationary states with two and three stripes at $\rho=55\%$ and 50%. States with a larger number of stripes can only survive in large systems, so we were not able to scan a broad enough range of system sizes L to determine an exponent. Since at sufficiently large scales there is an up-down symmetry in the case $n=2$, which is absent in the case $n=3$, where the boundary moves in one preferred direction, we expect different exponents.

The results for α and β are shown in Table III. Figure 18 shows the roughening of the boundary for the cases $n=2$ and $n=3$. The simulation results are compatible with the values $\alpha=1/2$ and $\beta=1/3$ for $n=3$ and $\alpha=1/2$ and $\beta=1/4$ for $n=2$, although other values cannot be ruled out. The former exponents are those of the Kardar-Parisi-Zhang universality class [20], whereas the latter belong to the Edwards-Wilkinson universality class [21], describing an interface in thermal equilibrium. For all $n \geqslant 3$, the boundaries exhibit a net movement in one preferred direction, thus breaking the up-down symmetry. Therefore, we expect to find the KPZ universality class also in the cases $n \geqslant 4$ that could not be investigated in the simulations.

In the limit of a large number of stripes $n \to \infty$, the movement of the infinite cluster is reminiscent of the movement of a front. To study the dynamics of such a front, we introduce a third state (''excited'') that marks the sites belonging to the front. The excitation spreads at each time step to all of its nearest occupied neighbors leaving behind an empty site. In order to ensure a constant density, one has to reoccupy randomly chosen empty sites. Starting with a flat excitation front in an initial state of average density ρ, after a short time either the front will have disappeared or the system will have evolved to a stationary state, where the front propagates quasideterministically in one direction. After leaving the system at one end, it reenters at the opposite end. Although the front state can be interpreted as a stripe state with $n=\infty$, there is one important difference. In the stripe state, the infinite cluster sees a medium with density below p_c in front of it, whereas in the front state, this density is above p_c. One therefore cannot expect to find KPZ behavior as in the stripe state. Instead, the shortest paths (using only occupied sites) from the sites of the front at time $t=0$ to the sites of the front at some later time have a Gaussian distribution, leading to a width of the interface that scales as $\ln(L)$, i.e., $\alpha=0$. Figure 19 shows the saturation width as function of the system size, together with a logarithmic fit.

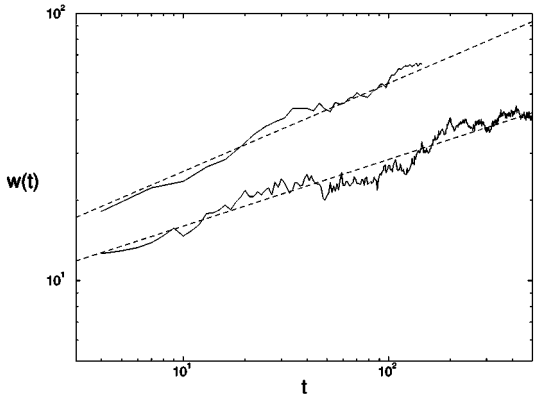

FIG. 18. Width w of the stripe boundary in the cases $n=2$ (lower curve) and $n=3$ (upper curve) for small t. The dashed lines have slope 1/4 and 1/3, respectively.

One can also compare this behavior with the behavior of an excitation front in a percolation system without periodic boundary conditions perpendicular to the front, i.e., a system

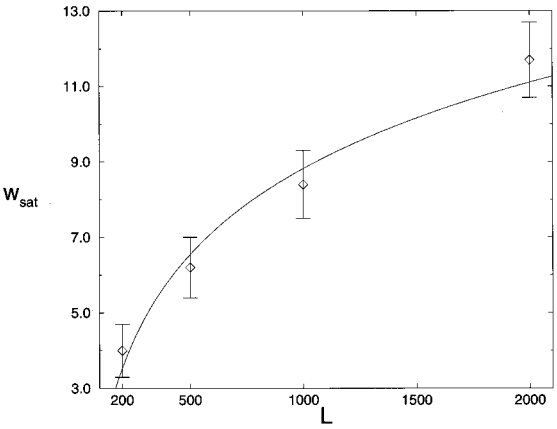

FIG. 19. Saturation width w_{sat} of an excitation front at $\rho=45\%$ and $\rho^{\mathrm{before}}=74\%$ ($L=200,500,1000,2000$). The smooth curve is a logarithmic fit.

of size L parallel to the front and of size ''∞'' perpendicular to it. The ''infinite'' extension perpendicular to the front would in practice be realized by providing a constant, homogeneous density ahead of the front, such that the front will never pass through a region where it already has been before, and additional correlations due to sites left over from the last passing are eliminated. In this case, the stability arguments of Sec. V A and of [18], which lead to the instability for $\rho^{\text{before}}<\rho^*$, are no longer valid, and one can investigate the properties of the front in the whole density interval of $\rho^{\text{before}}\in[p_c;1]$. Then one can also measure the exponent that describes how the velocity of the front vanishes when the density ρ^{before} approaches p_c. As in the preceding paragraph, we expect that such a front has a roughness exponent $\alpha=0$. Models that yield a front of finite roughness must therefore be more complicated and include a dependence of the front propagation on the shape of the front, or memory effects. Such models as the Kuramoto–Shivashinsky equation or the model in [22] give a KPZ roughness exponent.

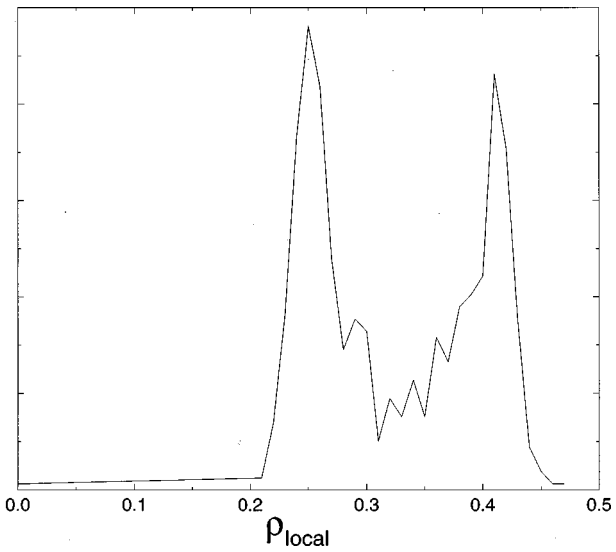

FIG. 20. Histogram of the local density ρ_{local} in a three-dimensional system for $L=100$ and $\rho\approx0.34$ in arbitrary units, averaged over 11^3 lattice sites.

VI. SUMMARY AND CONCLUSIONS

To conclude, we have described a nonequilibrium percolation model that shows several phenomena that are unknown in equilibrium percolation. Clusters of occupied sites are removed and refilled into the system at randomly chosen empty sites. For densities smaller than a critical density, there are only finite clusters, as in percolation theory. At the critical point, the critical exponents assume values different from percolation theory and they do not satisfy a hyperscaling relation. For densities between the critical density approximately equal to 40.8% and a second density approximately equal to 43.5%, the system remains critical, with the correlation length diverging slower than the system size. The value of the exponent that relates the correlation length with the system size depends on the density. For densities larger than approximately 43.5%, the system has a finite number of regions of different densities. The number of regions depends on the density and the transitions between states with different numbers of regions are discontinuous and show hysteresis. The shape of the regions is striped for periodic boundary conditions.

We were able to describe the dynamics of the system in the critical state as well as in the striped state in terms of patches of different densities. On length scales smaller than a ''finger thickness'' (critical region) or the stripe thickness (synchronized phase), the density of a patch is fairly homogeneous and goes through a temporal cycle: Starting from a small density, the density increases until most occupied sites of the patch are removed at $\rho\approx62.5\%$, and the cycle restarts. The system is therefore synchronized on small length scales. In the critical interval, the density is not large enough to allow a synchronization over the total width of the system, leading to the observed power laws. A similar relation between critical behavior and incomplete synchronization was found in the earthquake model [5]. There complete synchronization is hindered by the boundary conditions. In our model, the global density conservation prevents synchronization over distances larger than some correlation length. In both models, the correlation length diverges slower than the system size. A model with similar phenomena (i.e., subcritical, critical, and supercritical phases) has been reported in [23].

The density cycles observed in our model cannot exist in equilibrium systems, which are invariant under time reversal. Therefore, fluctuations in an equilibrium system are usually small and well described by a Gauss distribution around some mean value (except for the neighborhood of a critical point where the next-order terms have to be added to the free-energy functional). One consequence is the extensivity of equilibrium systems, i.e., a part of an equilibrium system behaves like a smaller system of the size of the part. This is not true for our model.

Although our simulations were performed in two dimensions, we expect the same general picture in higher dimensions: Unfortunately, in dimensions $d>2$, one has to cope with severe finite-size effects. For example, the three-dimensional analog of a two-stripe system would be a two-layer system. For this state to be stable, the correlation lengths in the layers have to be small compared to their thickness. With a given maximum number of sites approximately equal to 1.6×10^7 that could be simulated, the maximum thickness of one of two layers in a three-dimensional system is only approximately 125 compared to approximately 2000 in two dimensions. Another problem is that a visualization of the states like in two dimensions is not possible. One therefore has to measure local densities in order to determine the number of stripes that coexist in a given state. For the three-dimensional system, we could verify the transition to two stripes at $\rho^*_{3\text{D}}\approx0.34$. In Fig. 20, we plotted a histogram of the local density in a system at $\rho\lesssim\rho^*_{3\text{D}}$, proving the existence of two stripes.

We also simulated a variant where not an arbitrary site is selected, but always a site that belongs to the largest cluster in the system. The simulations were carried out for system sizes up to $L=1024$. Although the snapshots look different, since small clusters are no longer removed, we did not find different behavior. The important quantities, i.e., the critical exponents, $\rho_c^{(1)}$, $\rho_c^{(2)}$, and ρ^* remain the same.

An interesting modification of the model does not con-

serve the density of occupied sites exactly, but only on the average. While such a modification would not change the behavior of an equilibrium system, we expect some important changes in our model. When the density is not strictly conserved, large global density fluctuations can occur and a sharp distinction between a subcritical, a critical, and a supercritical phase is no longer possible. We plan to deal with this model in another paper [24].

The existence of these fundamental differences between equilibrium and many nonequilibrium systems makes it difficult to apply methods developed for the study of equilibrium critical behavior in nonequilibrium systems. It remains a challenge to find a field-theoretical formalism that allows one to analyze analytically the critical behavior of this and related models.

ACKNOWLEDGMENTS

S.C. was supported by the Deutsche Forschungsgemeinschaft Contract No. Schw 348/7-1. B.D. was supported by EPSRC Grant No. GR/K79307.

[1] P. Bak, C. Tang, and K. Wiesenfeld, Phys. Rev. Lett. **59**, 381 (1987).
[2] Z. Olami, H. J. S. Feder, and K. Christensen, Phys. Rev. Lett. **68**, 1244 (1992).
[3] B. Drossel and F. Schwabl, Phys. Rev. Lett. **69**, 1629 (1992).
[4] P. Bak and K. Sneppen, Phys. Rev. Lett. **71**, 4083 (1993); M. Paczuski, S. Maslov, and P. Bak, Phys. Rev. E **53**, 414 (1995).
[5] A. A. Middleton and C. Tang, Phys. Rev. Lett. **74**, 742 (1995).
[6] S. Lise and H. J. Jensen, Phys. Rev. Lett. **76**, 2326 (1996).
[7] B. Drossel, Phys. Rev. Lett. **76**, 936 (1996).
[8] A. Honecker and I. Peschel, Physica A **239**, 509 (1997).
[9] S. Clar, B. Drossel, and F. Schwabl, Phys. Rev. Lett. **75**, 2722 (1995).
[10] C. L. Henley, Phys. Rev. Lett. **71**, 2741 (1993).
[11] P. Grassberger, J. Phys. A **26**, 2081 (1993).
[12] K. Christensen, H. Flyvbjerg, and Z. Olami, Phys. Rev. Lett. **71**, 2737 (1993).
[13] S. Clar, B. Drossel, and F. Schwabl, Phys. Rev. E **50**, 1009 (1994).
[14] D. Stauffer and A. Aharony, *Introduction to Percolation Theory* (Taylor and Francis, London, 1992).
[15] T. C. Chan, H. F. Chau, and K. S. Cheng, Physica A **222**, 185 (1995).
[16] B. Drossel, S. Clar, and F. Schwabl, Phys. Rev. Lett. **71**, 3739 (1993).
[17] M. Paczuski and P. Bak, Phys. Rev. E **48**, R3214 (1993).
[18] S. Clar, K. Schenk, and F. Schwabl, Phys. Rev. E **55**, 2174 (1997).
[19] A.-L. Barabasi and H. E. Stanley, *Fractal Concepts in Surface Growth* (Cambridge University Press, Cambridge, 1995).
[20] M. Kardar, G. Parisi, and Y.-C. Zhang, Phys. Rev. Lett. **56**, 889 (1986).
[21] S. F. Edwards and D. R. Wilkinson, Proc. R. Soc. London, Ser. A **381**, 17 (1982).
[22] N. Provatas, T. Ala-Nissila, M. Grant, K. R. Elder, and L. Piché, J. Stat. Phys. **81**, 737 (1995).
[23] Á. Corral, C. J. Pérez, and A. Díaz-Guilera, Phys. Rev. Lett. **78**, 1492 (1997).
[24] S. Clar, B. Drossel, K. Schenk, and F. Schwabl (unpublished).